Energy Loss of a Charged Particle Moving over a 2D Strongly Coupled Dusty Plasma

Lu-Jing Hou,[1,2] Z. L. Mišković,[2] Ke Jiang,[1] and You-Nian Wang[1,*]

[1]State Key Lab of Materials Modification by Beams, Department of Physics, Dalian University of Technology, Dalian, China 116023
[2]Department of Applied Mathematics, University of Waterloo, Waterloo, Ontario, Canada N2L 3G1

(Received 12 August 2005; published 29 June 2006)

We use molecular dynamics (MD) simulation to evaluate the energy loss of a charged projectile moving parallel to a two-dimensional strongly coupled dusty plasma and compare the results with those obtained from the quasilocalized charge approximation (QLCA) and the Vlasov-random phase approximation. Good agreement is found between the QLCA and MD results when the projectile-dust coupling is weak. In the opposite regime, nonlinear effects in the dust-layer response render the QLCA model increasingly inadequate for calculating the energy losses at low projectile speeds.

DOI: 10.1103/PhysRevLett.96.255005 PACS numbers: 52.27.Lw, 52.27.Gr, 52.65.Yy

Introduction.—The interactions of fast charged particles with solid, gas, and plasma targets constitute a long-standing problem in which the so-called stopping power is often found to be a particularly useful parameter to quantify the particle energy loss [1,2]. Recent interest in the particle interactions with the strongly coupled plasmas has been prompted by a steady growth of the area of strongly coupled Coulomb systems (SCCS). This is evidenced by the series of conferences on SCCS with an ever expanding transdisciplinary scope [3], covering a range of topics, such as astrophysics, heavy-ion driven inertial controlled fusion (ICF) [2], cooling of charged-particle beams by electrons, ion trapping in non-neutral plasmas, electrons in quantum dots, electrons above free surface of liquid helium, two-dimensional (2D) electron structures in condensed matter [4], and particularly the rapidly growing field of strongly coupled dusty plasmas (SCDP) [5].

Our motivation in this Letter stems mainly from increasing focus in recent years on the interactions between the moving charges and SCDPs [5–9], where two main effects have been observed: excitation of collective modes in dust layers in the form of easily recorded Mach cones [5,6], and the spontaneous acceleration [5,7] of external charged particles moving underneath 2D dust crystals, accompanied by heating and melting of these crystals [8,9]. While the former effect has been investigated extensively and is well understood at present [5,6], the effect of particle acceleration is experimentally well documented, but its precise mechanism still presents an open problem. Samsonov *et al.* [5] were the first to observe spontaneous acceleration of external particles, which could attain speeds in far excess of thermal speeds of the dust-crystal particles, suggesting that simple thermalization cannot be the mechanism. Next, Schweigert *et al.* [7] studied this acceleration experimentally and by a molecular dynamics (MD) simulation, and found that their observations can be reproduced when the simulation uses asymmetrical interaction between the external particle and the dust crystal. More recently, Ichiki *et al.* [8] and Ivanov and Melzer [9] studied experimentally heating and nonequilibrium melting of small 2D plasma crystals, induced by external particles moving beneath them. The latter group proposed a simple analytical model based on the ion-wake instability, with a conclusion essentially equivalent to that of Schweigert *et al.* [7].

The point we adopt here is that both the spontaneous acceleration of external particles and the heating of plasma crystals involve the energy exchange between these two systems, and the stopping power of external particles should provide an adequate measure of that energy transfer. To date, only one group has been actively contributing to the theoretical study of the energy loss problem in dusty plasmas [10,11]. It should be noted, however, that these studies [10,11] are mainly concerned with charged projectiles moving through the homogeneous one-dimensional (1D) or three-dimensional (3D) bulk dusty plasmas. More importantly, they are essentially based on the random phase approximation (RPA), which does not take into account the short-range correlation between the particles in the dust layer and is therefore neither strictly applicable to SCDPs, nor is it capable of describing the nonlinear effects in the dust-layer response [1,2,5].

We study here the energy losses of charged projectiles moving parallel to a 2D dust layer in a SCDP, based on both analytical theories and numerical simulation. Besides using the RPA in our analytical approach, we also study the popular quasilocalized charge approximation (QLCA) due to Kalman and Golden [12–14]. On the numerical side, we perform a first Brownian motion MD simulation of the charged-particle stopping in the SCDPs. Therefore, our simulation includes, in a consistent manner, both the correlation between the dust particles in the layer and the nonlinear effects in the polarization of the dust layer by the projectiles.

Analytical theory.—We consider a monolayer of highly charged dust particles immersed in a large volume of plasma. The displacements $\mathbf{r} = \{x, y\}$ of dust particles are confined to the plane $z = 0$ in a Cartesian coordinate system with $\mathbf{R} = \{x, y, z\}$, while both electrons and ions follow the Boltzmann statistics in the whole plasma. Under

these conditions, the role of the electrons and ions is reduced to furnishing a polarizable background, responsible for the Yukawa-like interparticle potential [13,14], $\phi(r) = [(Z_d e)^2/r]\exp(-r/\lambda_D)$, with Z_d the charge number on each particle, $e > 0$ the elementary charge, λ_D the linearized Debye length. [Details of our model are given in [15].] Such a system is characterized by the coupling parameter $\Gamma = (Z_d e)^2/(aT_d)$ and the screening parameter $\kappa = a/\lambda_D$, where $a = (\pi\sigma_d)^{-1/2}$ is the 2D Wigner-Seitz radius with σ_d being the equilibrium surface density of the dust layer. Moreover, the 2D dust-layer plasma frequency is $\omega_{pd} = [2\pi\sigma_d(eZ_d)^2/m_d\lambda_D]^{1/2}$, with m_d being the mass of a dust particle.

Next, consider a test particle (TP) with the charge density $eZ_t\delta(\mathbf{r} - \mathbf{v}t)\delta(z - h)$, carrying Z_t elementary charges and moving with velocity $\mathbf{v}$ over (or underneath) the dust layer at a constant height h. This TP interacts with the dust particles via a 3D Yukawa potential, giving rise to the external potential $\phi_{\text{ext}}(\mathbf{R}, t)$ [15]. By using the Fourier transform $\mathbf{R} \equiv \{\mathbf{r}, z\} \rightarrow \mathbf{K} \equiv \{\mathbf{k}, k_z\}$ and $t \rightarrow \omega$, one obtains the induced potential as [1,2] $\Phi_{\text{ind}}(\mathbf{K}, \omega) = [1/\varepsilon(k, \omega) - 1]\phi_{\text{ext}}(\mathbf{K}, \omega)$, from which the stopping power can be calculated using the definition $S(v) \equiv eZ_t\hat{\mathbf{v}} \cdot \frac{\partial\Phi_{\text{ind}}(\mathbf{R},t)}{\partial\mathbf{r}}|_{z=h,\mathbf{r}=\mathbf{v}t}$ with $\hat{\mathbf{v}} = \mathbf{v}/v$. The longitudinal dielectric response function of the 2D dust layer can be expressed in general as [16,17]: $\varepsilon(k, \omega) = 1 - \omega_0^2(k)/[\omega(\omega + i\gamma) - (\sigma_{d0}/m_d)G(k, \omega)]$, where $\omega_0^2(k) = \sigma_d\phi(k)k^2/m_d$ with $\phi(k) = 2\pi(Z_d e)^2/(k^2 + \lambda_D^{-2})^{1/2}$ being the 2D Fourier transform of $\phi(r)$, γ is a phenomenological damping factor (Epstein coefficient) accounting for the dust-neutral collisions, and $G(\mathbf{k}, \omega)$ is the so-called dynamic local field correction (DLFC) function to account for the short-range correlation effect beyond the mean-field RPA description [16,17]. Setting $G(\mathbf{k}, \omega) = 0$ recovers a simple RPA dielectric function in the plasmon pole approximation.

However, we treat here the correlation effects by means of the QLCA, which considers the short-time response limit where $G(\mathbf{k}, \omega \rightarrow \infty) \equiv D_L(\mathbf{k})$ can be expressed in terms of the equilibrium radial distribution function (RDF) of the dust layer, $g(\mathbf{r})$, or its Fourier transform $g(\mathbf{k})$, as follows [12–15]

$$D_L(\mathbf{k}) = \int \frac{d^2\mathbf{q}}{(2\pi)^2} \frac{(\mathbf{q} \cdot \mathbf{k})^2}{k^2} \phi(q)[g(|\mathbf{q} - \mathbf{k}|) - g(\mathbf{q})], \quad (1)$$

with the RDF determined numerically from the MD simulation. We note that our analytical approach can be generalized to other strongly coupled physical systems by adopting other treatments of the correlation effects, or by using different interaction potentials ϕ [3]. For example, instead of the Yukawa potential, one could use the interaction between dust particles which includes the nonlinear screening effects [18].

MD simulation.—Our MD simulation consists of two steps. First, we track the Brownian motions of $N = 1600$ charged dust particles in a rectangle with periodic boundary conditions until a thermal equilibrium is reached. The particles are initially randomly located and are allowed to interact with each other via Yukawa potential, with the strength of interaction fully characterized by Γ and κ. The Brownian motions are generated by an asymmetric molecular bombardment from the neutral gas, which is related to the neutral friction γ via the fluctuation-dissipation theorem. Details of this simulation technique are described elsewhere [15,19]. After the system reaches the equilibrium, an RDF is calculated by an ensemble average and then used in Eq. (1). In the second step, a charged TP is projected horizontally into the system at a constant height h over the dust layer with velocity $\mathbf{v}$. The details of the interactions between the TP and all dust particles are recorded. In particular, the force $\mathbf{F}_s$ exerted on the TP by the dust particles is measured directly, and a time and an ensemble average of this force is evaluated in each run. Since the interactions between the TP and the dust particles are symmetrical, $-\hat{\mathbf{v}} \cdot \mathbf{F}_s$ is actually the stopping power.

Results and discussion.—We consider the dusty argon plasma with parameters selected according to the relevant experiments [5]: bulk plasma density $n_0 = 1.0 \times 10^8\ \text{cm}^{-3}$, electron temperature $T_e = 3.0$ eV, the ion and the dust-particle temperatures $T_i = T_d = 0.1$ eV, while the mass density and the radius of dust particles are $\rho_d = 1.0\ g/\text{cm}^3$ and $r_d = 2.0\ \mu$m. We have found that variation of the discharge pressure p plays no substantial role in our simulations, so we fix it at typical value $p = 20$ Pa [5]. We vary the dust-particle charge Z_d and the density σ_d, which both characterize the state of the dust layer. A range of the Γ and κ values will be used in Figs. 1 and 2 covering phase transition from a liquid to crystal, based on the criterion $\Gamma\exp(-\kappa) > 135$ [20]. We also vary the parameters characterizing the projectile: its speed v, charge number Z_t, and the height h above the dust layer, which all determine the strength of the TP coupling with the dust layer, to be discussed in Figs. 3 and 4.

In Fig. 1 we show the stopping power S (normalized by $S_n = T_e/\lambda_D$) versus the speed v, obtained from the MD simulation, and the QLCA and RPA models, for different coupling strengths Γ. All displayed data exhibit characteristic hill shapes with peaks at the TP speeds around the dust acoustic speed v_s, indicating the onset of resonance effects [1,2]. The difference between the peak positions in the curves shown in Fig. 1 is easily explained by $v_s^{\text{QLCA}} < v_s^{\text{RPA}}$ [13,14]. One of the most pronounced features in Fig. 1 is that the QLCA results agree very well with those from the MD simulations at all speeds, whereas the low-speed losses are heavily suppressed in the RPA. This deficiency of the RPA results is seen to increase with Γ, as expected on the account of the correlation effects [1,2]. In Fig. 1, we show the MD results for TPs with two opposite charges, $Z_t = \pm Z_d$, in order to assess the so-called Barkas effect due to nonlinear effects in the target response. One sees that the $Z_t = Z_d$ data tend to lie higher than the $Z_t = -Z_d$ points in the low-speed region, whereas

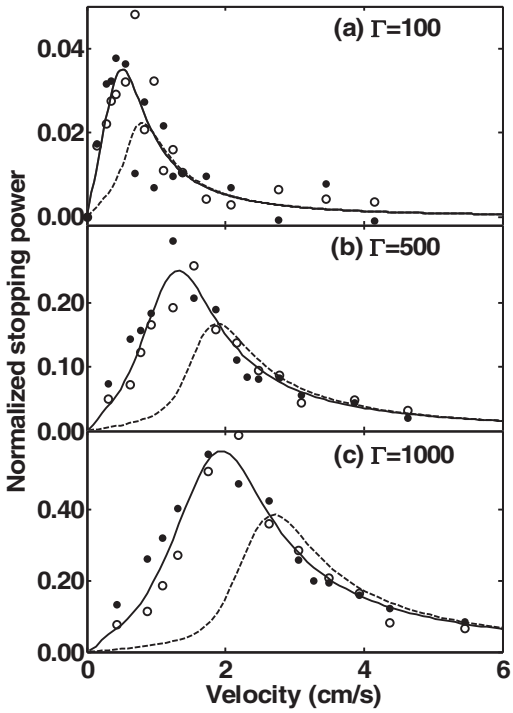

FIG. 1. Normalized stopping power vs projectile speed for: (a) $\Gamma = 100$, (b) $\Gamma = 500$, and (c) $\Gamma = 1000$, with $\kappa = 1$, $h = 1.6\lambda_D$, and $Z_t = (\pm)Z_d$ fixed. Solid and dashed lines show, respectively, the QLCA and RPA results, while the filled and empty circles show the MD data for, respectively, $Z_t = Z_d$ and $Z_t = -Z_d$.

in the high speed region they tend to merge, which is characteristic of the Barkas effect [4]. Given that both the RPA and the QLCA models are essentially linear-response theories, it is remarkable that the QLCA curve interpolates fairly well between the MD data for the two charge signs, as shown in Fig. 1, indicating that the nonlinear-response

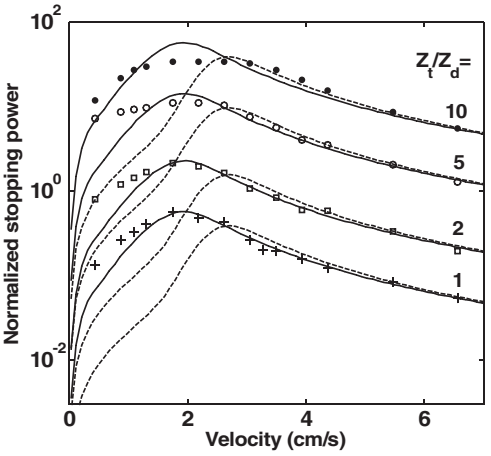

FIG. 3. Normalized stopping power vs projectile speed for $Z_t/Z_d = 1$, 2, 5, and 10, with $\Gamma = 1000$, $\kappa = 1$, and $h = 1.6\lambda_D$ fixed. Solid lines, dashed lines, and symbols indicate, respectively, the QLCA, RPA, and MD results.

effects are less pronounced compared to the strong coupling effects within the dust layer, at least for the range of parameters used in Fig. 1.

In Fig. 2, we show the effects of varying the screening parameter κ on stopping powers obtained from the QLCA and MD. One again notices a good agreement between the two sets of data at all speeds, except at the low-speed part for the largest screening parameter value, $\kappa = 2$. This discrepancy is a consequence of nonlinear effects in the target response, which we investigate next. In order to assess the effects of the coupling strength between the TP and dust particles, we adopt the parameter $\Theta(h, r, v) = V_{td}/(V_{dd} + m_d v^2/2)$, similar to the definition given in Ref. [2], where $V_{td} = |Z_t Z_d| e^2 \exp(-h/\lambda_D)/h$ is the maximum of the interaction energy between the TP and dust particles, and $V_{dd} = Z_d^2 e^2 \exp(-\kappa)/a$ is an average interaction energy within the dust layer. Since weak cou-

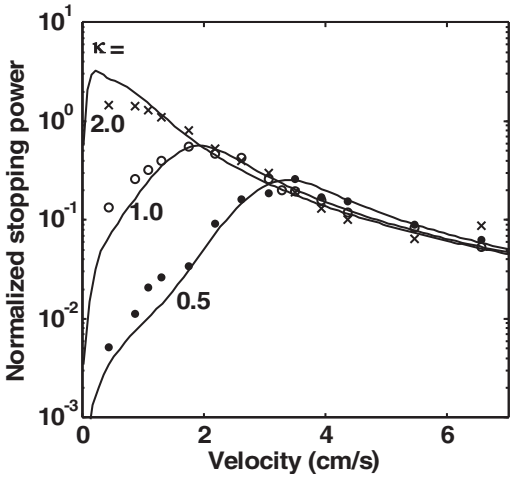

FIG. 2. Normalized stopping power vs projectile speed for $\kappa = 0.5$, 1.0, and 2.0, with $\Gamma = 1000$, $h = 1.6\lambda_D$, and $Z_t = Z_d$ fixed. Solid lines and symbols indicate, respectively, the QLCA and MD results.

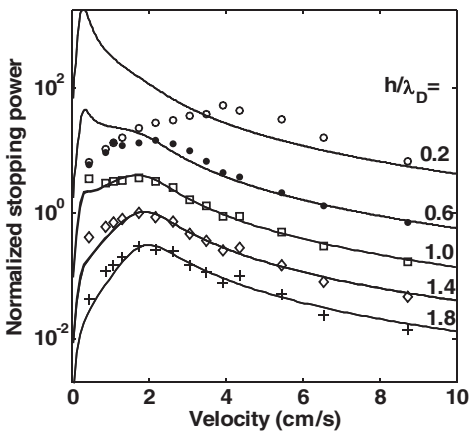

FIG. 4. Normalized stopping power vs projectile speed for $h/\lambda_D = 0.2$, 0.6, 1.0, 1.4, and 1.8, with $\Gamma = 1000$, $\kappa = 1$, and $Z_t = Z_d$ fixed. Solid lines and symbols indicate, respectively, the QLCA and MD results.

pling is realized for $\Theta \ll 1$, the value of $\Theta \approx 0.34$ for $v = 0$, corresponding to the data shown in Fig. 1, explains the good agreement between the QLCA and MD data observed in that figure. Similarly, in Fig. 2, we find $\Theta > 1$ only for $v < 1$ cm/s in the case with $\kappa = 2$, which describes well the onset of the nonlinear effects seen in that figure. To further test the performance of the QLCA against the nonlinear-response effects in the dust layer, we investigate next the effects of either increasing Z_t or decreasing h.

In Fig. 3, we compare the dependences of the stopping power on the projectile speed from the QLCA, RPA, and MD methods, for several values of the ratio Z_t/Z_d [1,2,4]. At higher TP charges, the MD data display a rounding of the main stopping peak of the QLCA curves, but the agreement between the MD and QLCA data remains good at supersonic speeds, which is also true for the RPA data. It is interesting to note that $\Theta < 1$ in all cases shown in Fig. 3, except when $v < 1.57$ cm/s for $Z_t/Z_d = 5$ and when $v < 2.90$ cm/s for $Z_t/Z_d = 10$, which seem to delineate the regions of a more substantial discrepancy between the QLCA and MD data. In addition, we have found from the MD data that the stopping power scales as $(Z_t/Z_d)^\chi$ with $1.7 \leq \chi \leq 2.0$ at low speeds, and with $\chi \approx 2.0$ for $v > 3v_s$. All this confirms that the linear models work well for sufficiently high projectile speeds, as shown previously for ion stopping in the ICF plasmas [2] and in the 2D degenerate electron gas [4].

In Fig. 4, we show the effects of changing the projectile distance from the dust layer on stopping powers calculated by the QLCA and MD methods. While the agreement between the QLCA and MD data is very good at all speeds for distances $h \geq a$, this agreement deteriorates spectacularly when the projectile gets closer to the dust layer than the average interparticle spacing $a\ (= \lambda_D)$ within that layer. The main peak in the MD data is seen to broaden and move to higher speeds for distances $h < a$, whereas the QLCA curves show the opposite trend in developing a sharp peak at a very low speed of about $v_* = 0.30$ cm/s so that, at the shortest distance $h = 0.2\lambda_D$, any signature of the main peak at the sound speed is lost. It is interesting that $\Theta < 1$ for all cases in Fig. 4, except when $v < 2.27$ cm/s for $h = 0.6\lambda_D$ and when $v < 5.92$ cm/s for $h = 0.2\lambda_D$, which are roughly the regions of the largest discrepancy between the QLCA and MD data. As before, the QLCA curves follow closely the MD data at high speeds, except for the shortest distance h, which is also true for the RPA curves (not shown in Fig. 4). Given that both linear models of stopping are essentially based on the collective excitation modes, we believe that the peak structure at around v_*, seen in the QLCA curves in Fig. 4, results from a relative amplification of the short-wavelength response of the dust layer for short distances h, which then brings up the effects of the local minima observed in the dispersion curves for the dust-layer collective modes [13,14]. This clearly shows inadequacy of using the *equilibrium* RDF in the QLCA for the purpose of calculating the energy losses of slow projectiles moving close, or within the dust layer.

Conclusion.—Our work presents a combined analytical and numerical analysis of the energy losses of charged particle moving over a 2D strongly coupled dusty plasma, with a special attention paid to the roles played by the coupling parameter Γ, the screening parameter κ, the projectile charge Z_t, and its distance h from the dust layer. The main conclusion is that the QLCA results for the projectile stopping power agree well with those of the MD simulations at all projectile speeds, and for a broad range of the Γ and κ values covering both the crystal and liquid state of the layer, as long as the projectile coupling to the dust layer is weak. On the other hand, as Z_t/Z_d increases and h decreases, nonlinear-response effects show up in the MD data, rendering the QLCA increasingly inadequate at low projectile speeds. In particular, when the projectile distance h from the dust layer is smaller than the interparticle separation a within this layer, the use of equilibrium RDF in Eq. (1) is not justified, as it cannot describe the single-particle excitation mechanism of the energy transfer to the dust system.

Support from the DPHE of China (Y. N. W) as well as from NSERC and PPER (Z. L. M) are acknowledged. The authors wish to thank Prof. Z. Donkó for valuable discussions

*Electronic address: ynwang@dlut.edu.cn

[1] D. Kremp, M. Schlanges, and W.-D. Kraeft, *Quantum Statistics of Nonideal Plasmas* (Springer, New York, 2005).
[2] G. Zwicknagel *et al.*, Phys. Rep. **309**, 117 (1999).
[3] V. E. Fortov *et al.*, preface to J. Phys. A **39**, No. 17 (2006).
[4] E. Zaremba *et al.*, Phys. Rev. Lett. **90**, 046801 (2003).
[5] D. Samsonov *et al.*, Phys. Rev. Lett. **83**, 3649 (1999).
[6] D. Dubin, Phys. Plasmas **7**, 3895 (2000).
[7] V. A. Schweigert *et al.*, Phys. Plasmas **9**, 4465 (2002).
[8] R. Ichiki *et al.*, Phys. Rev. E **70**, 066404 (2004).
[9] Y. Ivanov and A. Melzer, Phys. Plasmas **12**, 072110 (2005).
[10] M. H. Nasim *et al.*, Phys. Plasmas **7**, 762 (2000).
[11] S. Ali *et al.*, Phys. Plasmas **12**, 072104 (2005).
[12] G. J. Kalman and K. I. Golden, Phys. Rev. A **41**, 5516 (1990); K. I. Golden and G. J. Kalman, Phys. Plasmas **7**, 14 (2000).
[13] G. J. Kalman *et al.*, Phys. Rev. Lett. **84**, 6030 (2000).
[14] G. J. Kalman *et al.*, Phys. Rev. Lett. **92**, 065001 (2004).
[15] K. Jiang *et al.*, Phys. Rev. E **73**, 016404 (2006).
[16] M. S. Murillo and D. O. Gericke, J. Phys. A **36**, 6273 (2003).
[17] S. Ichimaru *et al.*, Phys. Rep. **149**, 91 (1987).
[18] V. N. Tsytovich *et al.*, Phys. Plasmas **13**, 033503 (2006).
[19] X. H. Zheng and J. C. Earnshaw, Phys. Rev. Lett. **75**, 4214 (1995).
[20] S. Nunomura *et al.*, Phys. Rev. Lett. **94**, 045001 (2005).